Mon. Not. R. Astron. Soc. **000**, 1–9 (2010) Printed 27 July 2010 (MN LaTeX style file v2.2)

General relativistic polarized radiative transfer: the interface between dynamics and observations

Roman V. Shcherbakov[1⋆]† and Lei Huang[2],[3],[4]
[1] *Harvard-Smithsonian Center for Astrophysics, 60 Garden Street, Cambridge, MA 02138, USA*
[2] *Academia Sinica, Institute of Astronomy and Astrophysics, Taipei 106, Taiwan*
[3] *Key Laboratory for Research in Galaxies and Cosmology, Shanghai Astronomical Observatory, Shanghai 200030, China*
[4] *Key Laboratory for Research in Galaxies and Cosmology, The University of Sciences and Technology of China, Hefei 230026, China*

27 July 2010

ABSTRACT

The rising amount of polarized observations of relativistic sources requires the correct theory for proper model fitting. The equations for general relativistic (GR) polarized radiative transfer are derived starting from the Boltzmann equation and basic ideas of general relativity. The derivation is aimed at providing a practical guide to reproducing the synchrotron part of radio & sub-mm emission from low luminosity active galactic nuclei (LLAGNs), in particular Sgr A*, and jets. The recipe for fast exact calculation of cyclo-synchrotron emissivities, absorptivities, Faraday rotation and conversion coefficients is given for isotropic particle distributions. The multitude of physical effects influencing simulated spectrum is discussed. The application of the prescribed technique is necessary to determine the black hole (BH) spin in LLAGNs, constraining it with all observations of total flux, linear and circular polarization fractions, and electric vector position angle as functions of the observed frequency.

Key words: black hole physics – Galaxy: centre – plasmas – polarization – radiation mechanisms: general – radiative transfer

1 INTRODUCTION

The good model of radiative transfer is the key in bridging the plasma dynamics and the observations of compact accreting sources. The dynamics of plasma evolved from hydrodynamics (Ruffert 1994) to magneto hydrodynamics (MHD) (Hawley & Balbus 2002) and particle-in-cell (PIC) simulations (Sironi & Spitkovsky 2009). The modelling of compact object's gravity has turned from quasi-Newtonian potential (Igumenshchev & Narayan 2002) to the full general relativistic (GR) MHD (Shafee et al. 2008). Only GRMHD simulations allow to fully account for the spin of the compact object. The radiative transfer approximations were improving as well. The simple quasi-Newtonian ray propagation (Chan et al. 2009) gave way to null-geodesics tracing in Kerr metric (Moscibrodzka et al. 2009). The huge amount of polarization observations demanded the polarized radiative transfer.

The main principles of GR polarized radiative transfer were formulated in Broderick (2004). However, that formulation was not ready for applications as it lacked, for example, the Faraday conversion and the suppression of Faraday rotation in hot plasmas. The first application to the real object was done in Huang et al. (2009). Their calculations included Faraday conversion, but made several approximations, some of which can be substantially improved upon. For example, their simple relation on V and Q emissivities and Faraday rotation and conversion constitutes an approximation that almost never holds. Their emissivities are calculated in synchrotron regime, which breaks for temperatures about the electron mass. Their frame of plasma does not fully account for the fluid motion. We are improving on their work in the present paper, in particular treating exactly the plasma response and extending it to non-thermal particle distributions.

Another important issue is the complexity of GR polarized radiative transfer. The errors and implicit strong approximations may slip into the equations of almost every author. This is more likely the case, when certain derivation is done half-way by one author and then continued by another author, e.g. the derivation of the Faraday conversion coefficient in the mixture of thermal and non-thermal plasmas in Melrose (1997) and Ballantyne, Ozel & Psaltis (2007) neglected the importance of the finite ratio of cyclotron to observed frequencies. Another good example is the definition of the sign of circular polarization V. It varies

⋆ E-mail: rshcherbakov@cfa.harvard.edu
† http://www.cfa.harvard.edu/%7Ershcherb/

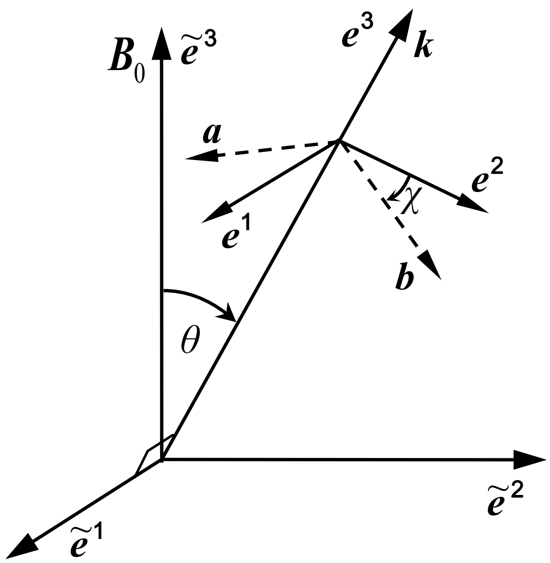

Figure 1. Geometry of the problem. Vector $\boldsymbol{B}_0$ represents uniform magnetic field. The transverse plane wave travels along $\boldsymbol{k}$ and has electric field $\boldsymbol{E}$ oscillating in $(\boldsymbol{e}^1\boldsymbol{e}^2)$ plane. Vectors $\boldsymbol{a}$ and $\boldsymbol{b}$ represent parallel transported basis orthogonalized with $\boldsymbol{k}$.

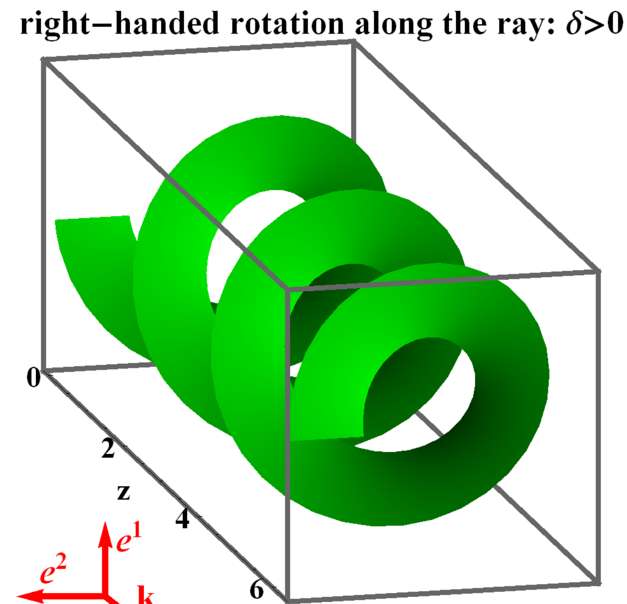

Figure 2. Right-handed rotation of electric field along the ray at fixed time t corresponding to negative circular polarized wave $V < 0$. Electric field is $E_1 = E_{1\omega}\exp(\imath(kz+\delta))$, $E_2 = E_{2\omega}\exp(\imath kz)$, $\delta = \pi/2$, where $E_{1\omega}$ is along $\boldsymbol{e}^1$, $E_{2\omega}$ along $\boldsymbol{e}^2$, and the wave propagates along $\boldsymbol{k}$. Vectors $\boldsymbol{e}^1$, $\boldsymbol{e}^2$, $\boldsymbol{k}$ constitute the right-handed triad.

from article to article and the consistent definition in a single derivation is essential.

Therefore, there appeared a need for the present paper. In a single derivation from the basic principles we provide the necessary applied expressions for GR polarized radiative transfer. We start in §2 by consistently defining the polarization tensor, Stokes parameters, and plasma response tensor and incorporating the response tensor into the Newtonian radiative transfer. In §3 we recast the derivation of the response tensor from Boltzmann equation for general isotropic particle distribution and do the special case of thermal distribution. We provide the applied expressions for response tensor in the plane perpendicular to the ray and give the consistent sign notation for both positive and negative charges in §3.3. The resultant formulas for absorptivities/emissivities, Faraday rotation and conversion coefficients are exact and easy to evaluate. By means of locally-flat co-moving reference frame we extend the radiative transfer to full GR in §4. We highlight the various physical effects important for real astrophysical objects in §5. Finally, in §6 we briefly summarize the methods and the ways to generalize them even further.

2 NEWTONIAN POLARIZED RADIATIVE TRANSFER

The proper treatment of polarization of radiation is necessary to take the full advantage of polarized observations. Let us start formulating the dynamics of polarization by defining the basis. Let $\tilde{\boldsymbol{e}}^3$ be the direction of uniform magnetic field $\boldsymbol{B}_0$. Then define the orthonormal triad $\boldsymbol{k}$, $\boldsymbol{e}^1$, and $\boldsymbol{e}^2$ in the standard way (Rybicki & Lightman 1979; Sazonov 1969; Pacholczyk 1970): wave propagates along $\boldsymbol{k}$ vector,

$$\boldsymbol{e}^1 = C(\boldsymbol{B}_0\times\boldsymbol{k}), \qquad (1)$$

$$\boldsymbol{e}^2 = \boldsymbol{k}\times\boldsymbol{e}^1,$$

where the scalar C can have either sign. We choose the axes as on Fig. 1: $\boldsymbol{e}^1$ is perpendicular to $(\boldsymbol{B}_0,\boldsymbol{k})$ plane and $\boldsymbol{B}_0$ lies in $(\boldsymbol{k},\boldsymbol{e}^2)$ plane. The rotation around $\boldsymbol{e}^1$ transforms basis $(\tilde{\boldsymbol{e}}^1, \tilde{\boldsymbol{e}}^2, \tilde{\boldsymbol{e}}^3)$ to the basis $(\boldsymbol{e}^1, \boldsymbol{e}^2, \boldsymbol{e}^3)$ as

$$\boldsymbol{e}^1 = \tilde{\boldsymbol{e}}^1,\quad \boldsymbol{e}^2 = \tilde{\boldsymbol{e}}^2\cos\theta - \tilde{\boldsymbol{e}}^3\sin\theta, \qquad (2)$$
$$\boldsymbol{e}^3 = \boldsymbol{k} = \tilde{\boldsymbol{e}}^2\sin\theta + \tilde{\boldsymbol{e}}^3\cos\theta,$$

which can be conveniently written as

$$\boldsymbol{e}^k = \tilde{\boldsymbol{e}}^i \mathsf{S}_{ik},\quad \mathsf{S}_{ik} = \begin{pmatrix} 1 & 0 & 0 \\ 0 & \cos\theta & \sin\theta \\ 0 & -\sin\theta & \cos\theta \end{pmatrix}. \qquad (3)$$

Vectors and tensors then rotate according to

$$A_k = (\mathsf{S}^T)_{ki}\tilde{A}_i,\quad \alpha_{ki} = (\mathsf{S}^T)_{km}\tilde{\alpha}_{mn}\mathsf{S}_{ni}, \qquad (4)$$

where $()^T$ is a transposed matrix. The angle θ can be found from

$$\cos\theta = \frac{\boldsymbol{k}\cdot\boldsymbol{B}_0}{kB_0}. \qquad (5)$$

For the electric field components E_1 along $\boldsymbol{e}^1$ and E_2 along $\boldsymbol{e}^2$ the Stokes parameters are defined as

$$\begin{aligned} I &= \langle E_1E_1^*\rangle + \langle E_2E_2^*\rangle, \\ Q &= \langle E_1E_1^*\rangle - \langle E_2E_2^*\rangle, \\ U &= \langle E_1E_2^*\rangle + \langle E_2E_1^*\rangle, \\ V &= \imath(\langle E_1E_2^*\rangle - \langle E_2E_1^*\rangle), \end{aligned} \qquad (6)$$

where the last formula chooses the IAU/IEEE definition (Hamaker & Bregman 1996) of V, actively used by observers. That is for positive V the rotation of electric field

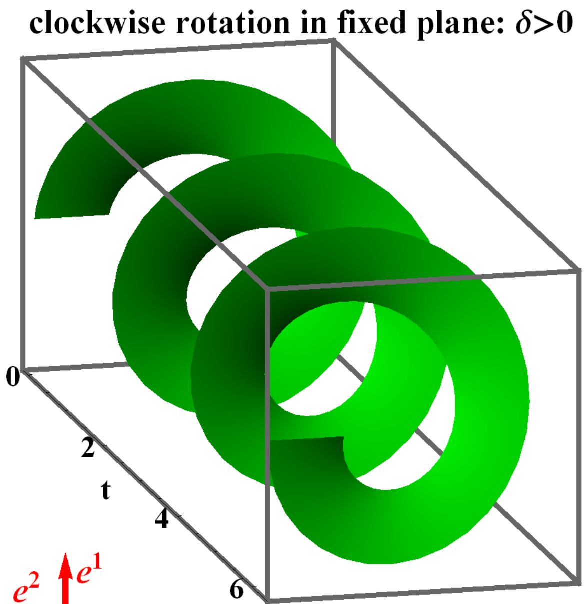

Figure 3. Left-handed rotation of electric field at fixed coordinate z with time corresponding to negative circular polarized wave $V<0$. Electric field is $E_1 = E_{1\omega}\exp(\imath(-\omega t+\delta))$, $E_2 = E_{2\omega}\exp(-\imath\omega t)$, $\delta=\pi/2$, where $E_{1\omega}$ is along $\boldsymbol{e}^1$, $E_{2\omega}$ along $\boldsymbol{e}^2$.

is counter-clockwise as seen by the observer. Nevertheless, all astrophysics textbooks agree on the opposite definition of V (Sazonov & Tsytovich 1968; Legg & Westfold 1968; Rybicki & Lightman 1979; Rochford 2001; Wilson et al. 2009). Let us visualize the electric field rotation. Take the electric field

$$E_1 = E_{1\omega}\exp(\imath(kz-\omega t+\delta)), \quad E_2 = E_{2\omega}\exp(\imath(kz-\omega t)) \tag{7}$$

with positive amplitudes (Fourier coefficients) $E_{1\omega}, E_{2\omega} > 0$ and substitute it to the definition (6). Then

$$\begin{aligned} I &= E_{1\omega}^2 + E_{2\omega}^2, \qquad Q = E_{1\omega}^2 - E_{2\omega}^2 \\ U &= 2E_{1\omega}E_{2\omega}\cos\delta, \quad V = -2E_{1\omega}E_{2\omega}\sin\delta \end{aligned} \tag{8}$$

and $V<0$ for $\delta\in(0,\pi)$. Let us fix time $t=0$, $\delta=\pi/2$ and draw the electric field vector in space along the ray (see Fig. 2). We see that the electric field corresponds to a right-handed screw. However, if we fix a plane in space by setting $z=0$ and draw the evolution of the electric field vector, then the rotation direction is the opposite: electric field vector rotates counter-clockwise, if viewed along the ray (see Fig. 3). These opposite directions of rotation is a common point of confusion (Rochford 2001). Correspondingly, the observer sees the clockwise-rotating electric field for $\delta=\pi/2$, as she is situated at a fixed z, and counter-clockwise rotating electric field for $\delta=-\pi/2$ and positive $V>0$. The definition (6) of V has a marginal advantage: the electrons generate positive V for propagation along the magnetic field. Let us take an electron on a circular orbit in $(\tilde{\boldsymbol{e}}^1\tilde{\boldsymbol{e}}^2)$ plane. It moves from the direction of $\tilde{\boldsymbol{e}}^1$ to the direction of $\tilde{\boldsymbol{e}}^2$, id est clockwise as viewed along the magnetic field. Then the wake of the electric field follows the charge and rotates clockwise. The resultant wave propagates along $\boldsymbol{B}_0$ and constitutes a left-handed screw, which gives the positive $V>0$.

The polarization tensor is obtained automatically from equation (6) as

$$I_{ij} = \left\langle E_i E_j^* \right\rangle = \frac{1}{2}\begin{pmatrix} I+Q & U-\imath V \\ U+\imath V & I-Q \end{pmatrix}. \tag{9}$$

The polarization vector is

$$\boldsymbol{S} = (I,Q,U,V)^T. \tag{10}$$

Note that Melrose & McPhedran (1991) uses the same definitions, however, their $\boldsymbol{k}$, $\boldsymbol{e}^1$, $\boldsymbol{e}^2$ constitute a left triad instead of a right triad.

The plasma response is characterized by the 4×4 response tensor $\alpha^\mu{}_\nu$

$$j^\mu_\omega = \alpha^\mu{}_\nu A^\nu_\omega \tag{11}$$

as the proportionality between the four-vectors of vector potential amplitude and the current density amplitude. There is freedom in choosing the gauge condition for A^μ. Let us choose the Lorenz gauge

$$A^\mu u_\mu = 0 \tag{12}$$

at each point along the ray and enforce it by adding to A^μ a vector, proportional to k^μ, what does not change the polarization tensor (9) (Misner, Thorne & Wheeler 1973). The gauge condition makes $A^0=\phi=0$ and establishes the proportionality of wave electric field $\boldsymbol{E}$ and $\boldsymbol{A}$ in the locally flat co-moving frame (Anile & Breuer 1974; Landau & Lifshitz 1975). Thus, in that frame the spatial components of $\alpha^\mu{}_\nu$ coincide exactly with the spatial 3×3 response tensor α_{ik} in $(j_\omega)_i = \alpha_{ik}(A_\omega)_j$. We will derive the tensor α_{ik} below. It is usually incorporated within the dielectric tensor

$$\varepsilon_{ik} = \delta_{ik} + \frac{4\pi c}{\omega^2}\alpha_{ik}. \tag{13}$$

The wave equation for transverse waves in terms of ε_{ik} is

$$(n_{\rm r}^2\delta_{ik} - \varepsilon_{ik})\begin{pmatrix} E_1 \\ E_2 \end{pmatrix} = 0, \tag{14}$$

where the indices $i,k=1,2$, so that only the transverse 2×2 part of ε_{ik} in $(\boldsymbol{e}^1, \boldsymbol{e}^2, \boldsymbol{k})$ basis is taken, and $n_{\rm r}^2 = k^2c^2/\omega^2$ (Swanson 2003; Shcherbakov 2008). The correspondent transport equation is (Melrose & McPhedran 1991)

$$\frac{dE_i}{ds} = \frac{\imath\omega}{2n_{\rm r}c}\Delta\varepsilon_{ik}E_k, \tag{15}$$

where $\Delta\varepsilon_{ik} = \varepsilon_{ik}-\delta_{ik}$. We take the equation (15), its conjugate, multiply correspondingly by E_k^* and E_k, add and obtain

$$\frac{d\left\langle E_iE_k^*\right\rangle}{ds} = \frac{\imath}{\nu}(\alpha_{il}\left\langle E_lE_k^*\right\rangle - \alpha_{kl}^*\left\langle E_iE_l^*\right\rangle) \tag{16}$$

for $n_{\rm r}=1$ neglecting emission. Again, $i,k,l=1,2$. Note that $\alpha_{12}=-\alpha_{21}$ according to Onsager principle (Landau & Lifshits 1980) (p. 273). By solving the definitions of the Stokes parameters (eq. (6)) for $\langle E_iE_k^*\rangle$ and substituting the result into the equation (16) we get the transport equation for the Stokes parameters

$$\frac{d\boldsymbol{S}}{ds} = \begin{pmatrix} \varepsilon_I \\ \varepsilon_Q \\ 0 \\ \varepsilon_V \end{pmatrix} - \begin{pmatrix} \alpha_I & \alpha_Q & 0 & \alpha_V \\ \alpha_Q & \alpha_I & \rho_V & 0 \\ 0 & -\rho_V & \alpha_I & \rho_Q \\ \alpha_V & 0 & -\rho_Q & \alpha_I \end{pmatrix}\boldsymbol{S} \tag{17}$$

with the polarization $\boldsymbol{S}$ vector (10) by adding the emission, where

$$\begin{aligned}\alpha_I &= \mathrm{Im}(\alpha_{22}+\alpha_{11})/\nu,\\ \alpha_Q &= \mathrm{Im}(\alpha_{11}-\alpha_{22})/\nu,\\ \alpha_V &= 2\mathrm{Re}(\alpha_{12})/\nu,\\ \rho_V &= 2\mathrm{Im}(\alpha_{12})/\nu,\\ \rho_Q &= \mathrm{Re}(\alpha_{22}-\alpha_{11})/\nu.\end{aligned} \tag{18}$$

3 DERIVATION OF RESPONSE TENSOR

The response tensor is derived for thermal plasma in Trubnikov (1958); Melrose (1997); Swanson (2003). However, there is a need to recast the derivation, since we want to consider both signs of charge, extend the results to non-thermal isotropic particle distributions, and seek for extensions to non-isotropic distributions. The importance of notation consistency cannot be overemphasized, also the orientation of our coordinate axes is different from some of the above sources. On the way we discover the practical significance of the response tensor: it offers expressions for fast evaluation of plasma absorptivities and rotativities.

3.1 General isotropic particle distribution

Throughout this subsection and next subsection we employ vectors and tensors in ($\tilde{\boldsymbol{e}}^1$, $\tilde{\boldsymbol{e}}^2$, $\tilde{\boldsymbol{e}}^3$) basis, but skip tildes to avoid clutter. Only tildes over the response tensors are drawn. For simplicity of notation we define the dimensionless momentum

$$p=\sqrt{\gamma^2-1}, \tag{19}$$

where $\gamma=En/(mc^2)\geqslant 1$ is the γ-factor for particles of energy En and mass m. Then the Boltzmann equation is

$$\frac{\partial f}{\partial t}+\boldsymbol{v}\cdot\boldsymbol{\nabla}f+\eta e\left(\boldsymbol{E}+\frac{\boldsymbol{v}}{c}\times(\boldsymbol{B}_0+\boldsymbol{B})\right)\cdot\frac{\boldsymbol{\nabla}_p f}{mc}=0. \tag{20}$$

Here the velocity vector is

$$\boldsymbol{v}=\boldsymbol{p}c/\gamma, \tag{21}$$

$\boldsymbol{B}_0$ is the background magnetic field, $\boldsymbol{E}$ and $\boldsymbol{B}$ are the wave electric and magnetic fields, η is the sign of the charge and $e>0$. Let us assume a general isotropic particle distribution $f_0(p)$ instead of thermal. The wave with the phase $\exp(\imath(\boldsymbol{k}\cdot r-\omega t))$ causes perturbation in a form

$$f_1=\exp(\imath(\boldsymbol{k}\cdot r-\omega t))f_0\Phi(\boldsymbol{p}), \tag{22}$$

which implements the general function $\Phi(\boldsymbol{p})$ of momentum $\boldsymbol{p}$. Following Trubnikov (1958); Swanson (2003) we introduce the cylindrical coordinates with axis along $\boldsymbol{B}_0$, so that

$$p_x=p_\perp\cos\phi,\quad p_y=p_\perp\sin\phi \tag{23}$$

with angle ϕ in (xy) plane. Then

$$\boldsymbol{k}\cdot\boldsymbol{p}=k_z p_z+k_\perp p_\perp\sin\phi. \tag{24}$$

The Boltzmann equation (20) results in

$$\begin{aligned}-\imath\omega f_1 &+ \frac{\imath(k_z p_z+k_\perp p_\perp\sin\phi)c}{\gamma}f_1\\ &+ \eta e\boldsymbol{E}\cdot\frac{\boldsymbol{\nabla}_p f_0}{mc}+\frac{\eta e}{\gamma}(\boldsymbol{p}\times\boldsymbol{B}_0)\cdot\frac{\boldsymbol{\nabla}_p f_1}{mc}=0\end{aligned} \tag{25}$$

upon substitution of f_1 from equation (22). For general isotropic $f_0(p)$ the relation $(\boldsymbol{p}\times(\boldsymbol{B}_0+\boldsymbol{B}))\cdot\boldsymbol{\nabla}_p f_0=0$ holds, and it does not hold for non-isotropic distributions. Only the cylindrical ϕ component is non-zero in a triple product $(\boldsymbol{p}\times\boldsymbol{B}_0)\cdot\boldsymbol{\nabla}_p f_1$. After some transformations we obtain an equation on $\Phi(\boldsymbol{p})$

$$\begin{aligned}-\imath\omega\Phi &+ \frac{\imath(k_z p_z+k_\perp p_\perp\sin\phi)c}{\gamma}\Phi\\ &+ \frac{d\ln f_0}{d\gamma}\frac{\eta e}{\gamma mc}(\boldsymbol{p}\cdot\boldsymbol{E}_\omega)-\frac{\eta\omega_B}{\gamma}\frac{\partial\Phi}{\partial\phi}=0\end{aligned} \tag{26}$$

for general isotropic particle distribution, where $\boldsymbol{E}_\omega$ is a Fourier amplitude. Here the cyclotron frequency is

$$\omega_B=\frac{eB_0}{mc},\quad \nu_B=\frac{\omega_B}{2\pi}. \tag{27}$$

We define the ratio β

$$\beta=\frac{\nu_B}{\nu}. \tag{28}$$

Alternatively, the equation (26) reads

$$\imath(a-b\sin\phi)\Phi+\partial\Phi/\partial\phi=F \tag{29}$$

with

$$a=\frac{\gamma-n_z p_z}{\eta\beta},\quad b=\frac{n_\perp p_\perp}{\eta\beta},\quad F=\frac{d\ln f_0}{d\gamma}\frac{\boldsymbol{p}\cdot\boldsymbol{E}_\omega}{B_0}. \tag{30}$$

Here $n_z=\cos\theta$ and $n_\perp=\sin\theta$ assuming $|\boldsymbol{k}|c=\omega$. The solution is

$$\Phi(\phi)=\exp(-\imath(a\phi+b\cos\phi))\int_{\phi_0}^{\phi}\exp(\imath(a\psi+b\cos\psi))F(\psi)d\psi, \tag{31}$$

where the lower boundary ϕ_0 is chosen at $t=-\infty$. The negative charge moves in the positive ϕ direction and the positive charge in the negative ϕ direction, therefore $\phi_0=-\eta\infty$. The solution of a homogeneous equation vanishes over the finite time. Knowing the particle distribution we calculate the Fourier transform of the current density

$$\boldsymbol{j}_\omega=\eta e\int f_0\Phi(\boldsymbol{p})\frac{\boldsymbol{p}c}{\gamma}d^3p \tag{32}$$

and relate it to the electric field $\boldsymbol{E}_\omega$ and the vector potential $\boldsymbol{A}_\omega$ amplitudes of the wave as

$$(j_\omega)_i=\sigma_{ik}(E_\omega)_k=\alpha_{ik}(A_\omega)_k, \tag{33}$$

where $\alpha_{ik}=\imath\omega\sigma_{ik}/c$. Let us calculate α_{ik}. Substituting the solution (31) into the definition of the current density equation (32) and changing the integration variable as $\psi=\phi-\xi$ we get

$$\begin{aligned}(j_\omega)_i &= \imath\frac{\eta e\omega}{c}\int d^3p\int_0^{-\eta\infty}\exp(-\imath a\xi+\imath b(\cos(\phi-\xi)-\cos\phi))\\ &\times\ p_i\ \ (p_k(A_\omega)_k)_{\phi\to\phi-\xi}\frac{c}{\gamma B_0}\frac{df_0}{d\gamma}d\xi.\end{aligned} \tag{34}$$

One can (Trubnikov 1958; Landau & Lifshits 1980; Swanson 2003) introduce the differentiation with respect to vectors $\boldsymbol{s}$ and $\boldsymbol{s}'$ to eliminate the momenta $\boldsymbol{p}$ in the integral expressions, then due to uniform convergence of the integrals in $d\xi$ and dp move the derivatives outside the integrals. We also do the transformation $\xi\to-\eta\beta\xi$ to finally get in ($\tilde{\boldsymbol{e}}^1$, $\tilde{\boldsymbol{e}}^2$, $\tilde{\boldsymbol{e}}^3$) basis

$$\tilde{\alpha}_{ik}=-\frac{\imath e^2}{mc}\int d^3p\int_0^\infty\frac{\partial^2\exp(\imath\xi\gamma-\imath\boldsymbol{h}\cdot\boldsymbol{p})}{\partial s_i\partial s'_k}\frac{df_0}{\gamma d\gamma}d\xi \tag{35}$$

$$= -\frac{4\pi\imath e^2}{mc}\frac{\partial^2}{\partial s_i\partial s'_k}\int_1^\infty d\gamma\frac{df_0}{d\gamma}\int_0^\infty \exp(\imath\xi\gamma)\frac{\sin(hp)}{h}d\xi$$

with

$$\begin{aligned} h_x &= \frac{n_\perp}{\beta\eta}(1-\cos(\beta\xi)) + \imath(s_x+\cos(\beta\xi)s'_x+\eta\sin(\beta\xi)s'_y),\\ h_y &= \frac{\sin(\beta\xi)n_\perp}{\beta} + \imath(s_y-\eta\sin(\beta\xi)s'_x+\cos(\beta\xi)s'_y),\\ h_z &= \xi n_z + \imath(s_z+s'_z),\\ h &= \sqrt{h_x^2+h_y^2+h_z^2}. \end{aligned} \quad (36)$$

3.2 Thermal particle distribution

Let us now consider the special case of an isotropic thermal distribution of particles

$$f_0 = \frac{n_e}{4\pi}\frac{\exp(-\gamma/\theta_e)}{\theta_e K_2(\theta_e^{-1})} \quad (37)$$

normalized as

$$\int_0^{+\infty} f_0 4\pi p^2 dp = n_e. \quad (38)$$

The normalized particle temperature is

$$\theta_e = \frac{k_B T}{mc^2}. \quad (39)$$

Then the response tensor (35) is

$$\tilde{\alpha}_{ik} = \frac{\imath e^2 n_e}{mc}\int\int_0^\infty \frac{\partial^2}{\partial s_i\partial s'_k}\frac{\exp(-A'\gamma-\imath\boldsymbol{h}\cdot\boldsymbol{p})}{4\pi\gamma\theta_e^2K_2(\theta_e^{-1})}d\xi d^3p \quad (40)$$

with $A' = 1/\theta_e - \imath\xi$ and the rest of quantities defined by equation (36). The integral over d^3p can be taken analytically (Trubnikov 1958) to give

$$\tilde{\alpha}_{ik} = \frac{\imath e^2 n_e}{mc\theta_e^2K_2(\theta_e^{-1})}\frac{\partial^2}{\partial s_i\partial s'_k}\int_0^\infty \frac{K_1(\sqrt{A'^2+h^2})}{\sqrt{A'^2+h^2}}d\xi. \quad (41)$$

Performing the differentiation in Mathematica 7 to avoid errors, one gets 3×3 response tensor

$$\tilde{\alpha}_{ik} = \frac{\imath e^2 n_e}{mc\theta_e^2K_2(\theta_e^{-1})}\int_0^\infty d\xi\left(\tilde{T}^1_{ik}\frac{K_2(\mathcal{R})}{\mathcal{R}^2} - \tilde{T}^2_{ik}\frac{K_3(\mathcal{R})}{\beta^2\mathcal{R}^3}\right) \quad (42)$$

with

$$\mathcal{R} = \sqrt{\frac{1}{\theta_e^2} - \frac{2\imath\xi}{\theta_e} - \xi^2\sin^2\theta + \frac{2\sin^2\theta}{\beta^2}(1-\cos\beta\xi)}. \quad (43)$$

Here

$$\tilde{T}^1_{ik} = \begin{pmatrix} \cos\beta\xi & \eta\sin\beta\xi & 0\\ -\eta\sin\beta\xi & \cos\beta\xi & 0\\ 0 & 0 & 1 \end{pmatrix}, \quad (44)$$

$$\tilde{T}^2_{ik} = \begin{pmatrix} -(1-\cos\beta\xi)^2\sin^2\theta & \eta(1-\cos\beta\xi)\sin\beta\xi\sin^2\theta & \eta\beta\xi(1-\cos\beta\xi)\cos\theta\sin\theta\\ -\eta(1-\cos\beta\xi)\sin\beta\xi\sin^2\theta & \sin^2\beta\xi\sin^2\theta & \beta\xi\sin\beta\xi\sin\theta\cos\theta\\ -\eta\beta\xi(1-\cos\beta\xi)\cos\theta\sin\theta & \beta\xi\sin\beta\xi\sin\theta\cos\theta & \beta^2\xi^2\cos^2\theta \end{pmatrix}. \quad (45)$$

3.3 Rotation of thermal response tensor

Let us apply the transformation (4) to tensors $\tilde{T}^1_{ik}$ and $\tilde{T}^2_{ik}$ and take the transverse 2×2 part to obtain correspondingly

$$T^1_{ij} = \begin{pmatrix} \cos\beta\xi & \eta\sin\beta\xi\cos\theta\\ -\eta\sin\beta\xi\cos\theta & \cos\beta\xi\cos^2\theta+\sin^2\theta \end{pmatrix} \quad (46)$$

and $T^2_{ij} = R_i\bar{R}_j$ with

$$\begin{aligned} R_i &= \sin\theta(\eta(1-\cos\beta\xi), \cos\theta(\sin\beta\xi-\beta\xi)), \quad (47)\\ \bar{R}_j &= \sin\theta(-\eta(1-\cos\beta\xi), \cos\theta(\sin\beta\xi-\beta\xi)) \end{aligned}$$

for

$$\alpha_{ij} = \frac{\imath e^2 n_e}{mc\theta_e^2K_2(\theta_e^{-1})}\int_0^\infty d\xi\left(T^1_{ij}\frac{K_2(\mathcal{R})}{\mathcal{R}^2} - T^2_{ij}\frac{K_3(\mathcal{R})}{\beta^2\mathcal{R}^3}\right). \quad (48)$$

The integration over ξ converges very slowly, if performed along the real axis. The way to accelerate the convergence is to perform the integration in a complex plane at a positive angle to the real axis. The wave frequency ν in the above calculations has a small positive imaginary part $\mathrm{Im}(\nu) > 0$ to account for the energy pumped into particles from passing waves. Then $\mathrm{Im}(\beta) < 0$ and the expression (43) has zeros only in the lower plane $\mathrm{Im}(\xi) < 0$ of ξ. Thus, deforming the integration contour to the upper plane of ξ does not change the response tensor (48). Note that all absorptivities α_I, α_Q, and α_V and rotativities ρ_Q and ρ_V are positive for electrons for $\theta \in (0,\pi/2)$ under the definitions (18), what gives an easy way to check the implementation of radiative transfer algorithm. The evaluation of these coefficients will be reported in the subsequent paper (Huang & Shcherbakov (2010), in prep.).

Following Huang et al. (2009) we define the parallel transported vectors $\boldsymbol{a}$ and $\boldsymbol{b}$ in addition to the right triad $\boldsymbol{e}^1$, $\boldsymbol{e}^2$, $\boldsymbol{k}$, so that in the co-moving locally-flat reference frame

$$(\boldsymbol{a},\boldsymbol{b}) = (\boldsymbol{e}^1,\boldsymbol{e}^2)\begin{pmatrix} \cos\chi & \sin\chi\\ -\sin\chi & \cos\chi \end{pmatrix}. \quad (49)$$

Then the transformation with -2χ angle

$$\mathbf{R}(\chi) = \begin{pmatrix} 1 & 0 & 0 & 0\\ 0 & \cos(2\chi) & -\sin(2\chi) & 0\\ 0 & \sin(2\chi) & \cos(2\chi) & 0\\ 0 & 0 & 0 & 1 \end{pmatrix} \quad (50)$$

serves to get the vector of emissivities $\boldsymbol{\varepsilon}$ and the matrix of rotativities/absorptivities K in ($\boldsymbol{a}$, $\boldsymbol{b}$, $\boldsymbol{k}$) basis as

$$\begin{aligned} \boldsymbol{\varepsilon} &= \mathbf{R}(\chi)\begin{pmatrix} \varepsilon_I\\ \varepsilon_Q\\ 0\\ \varepsilon_V \end{pmatrix}, \quad (51)\\ \mathbf{K} &= \mathbf{R}(\chi)\begin{pmatrix} \alpha_I & \alpha_Q & 0 & \alpha_V\\ \alpha_Q & \alpha_I & \rho_V & 0\\ 0 & -\rho_V & \alpha_I & \rho_Q\\ \alpha_V & 0 & -\rho_Q & \alpha_I \end{pmatrix}\mathbf{R}(-\chi). \end{aligned}$$

Define the perpendicular magnetic field

$$\boldsymbol{B}_{0\perp} = \boldsymbol{B}_0 - \boldsymbol{k}(\boldsymbol{k}\cdot\boldsymbol{B}_0)/k^2. \quad (52)$$

The trigonometric factors are related to the magnetic field as

$$\sin\chi = (\boldsymbol{a}\cdot\boldsymbol{B}_{0\perp})/B_{0\perp}, \quad \cos\chi = -(\boldsymbol{b}\cdot\boldsymbol{B}_{0\perp})/B_{0\perp}. \quad (53)$$

The radiative transfer equation is then

$$d\boldsymbol{S}/ds = \boldsymbol{\varepsilon} - \mathbf{K}\boldsymbol{S} \quad (54)$$

for the polarization vector $\boldsymbol{S}$ defined in $(\boldsymbol{a}, \boldsymbol{b}, \boldsymbol{k})$ basis.

4 EXTENSION TO GENERAL RELATIVITY

Let us consider two reference frames: locally-flat co-moving reference frame with 4-velocity $\hat{u}^\alpha = (1,0,0,0)$ and flat metric and the lab frame with Kerr metric and the fluid moving at u^α. We denote by hats $\hat{()}$ the quantities in the co-moving frame. Consider the radiative transfer equation (54) in the co-moving frame. The set of Stokes parameters $\boldsymbol{S}$ can be generalized to the corresponding set of photon occupation numbers

$$\boldsymbol{N} = \boldsymbol{S}/\nu^3, \quad (55)$$

which are invariant under the orthogonal coordinate transformations (Misner, Thorne & Wheeler 1973; Anile & Breuer 1974; Ellis 2009). Photons propagate along null-geodesics with the affine parameter λ, so that the wave four-vector is

$$k^\alpha = \frac{dx^\alpha}{d\lambda}, \quad (56)$$

and

$$\frac{d\boldsymbol{N}}{d\lambda} = 0. \quad (57)$$

One calculates the null geodesic starting from the observer's plane. The perpendicular unit vector a^α has a special orientation on that plane, and is transported along geodesic according to

$$a^\alpha(\lambda=0) = a_0^\alpha, \quad a_0^\alpha a_{\alpha 0} = 1, \quad k^\sigma \nabla_\sigma a^\alpha = 0, \quad (58)$$

where ∇_σ is the covariant derivative. The unit vector b^α is transported the same way.

Just as in a flat space case the charged particles lead to the increase of occupation numbers $\boldsymbol{N}$ due to emission, to decrease of $\boldsymbol{N}$ due to absorption, and to exchange of $\boldsymbol{N}$ components due to Faraday rotation and Faraday conversion. These are all the processes occuring in linear regime. The invariant number of photons emitted per unit solid angle per unit frequency per unit volume per unit time is proportional to the invariant $\varepsilon(\nu)/\nu^2 = \hat{\varepsilon}(\hat{\nu})/\hat{\nu}^2$ (Mihalas & Mihalas 1984) as

$$\frac{d\boldsymbol{N}}{d\lambda} \propto \frac{\varepsilon(\nu)}{\nu^2}, \quad (59)$$

where

$$\nu = -k^\mu u_\mu \quad (60)$$

is the photon frequency in the lab frame for $(-,+,+,+)$ signature of metric. By $\hat{\nu}$ the photon frequency in the co-moving frame is denoted. The invariant change of photon states due to absorption and propagation effects is proportional to the co-moving frame matrix $\mathbf{K}$ (see eq.(54)) taken within unit frequency unit solid angle unit volume unit time. Thus the proportionality to the invariant $\nu\mathbf{K}(\nu) = \hat{\nu}\hat{\mathbf{K}}(\hat{\nu})$ is established (Mihalas & Mihalas 1984) as

$$\frac{d\boldsymbol{N}}{d\lambda} \propto -\nu\mathbf{K}(\nu)\boldsymbol{N}, \quad (61)$$

where the whole form of the absorption/state change matrix is preserved. The full GR radiative transfer equation

$$\nu_\infty \frac{d\boldsymbol{N}}{d\lambda} = \frac{\hat{\varepsilon}(\hat{\nu})}{\hat{\nu}^2} - \hat{\nu}\hat{\mathbf{K}}(\hat{\nu})\boldsymbol{N} \quad (62)$$

is obtained. Here the affine parameter is normalized to the observed frequency ν_∞, so that far from the BH $ds \approx d\lambda$. The equation (62) is similar to the GR polarized transfer equation in Huang et al. (2009). However, their usage of primed and unprimed quantities is potentially confusing. It is their primed quantity $\boldsymbol{S}'$, which should be generalized to GR as $\boldsymbol{N}_S = \boldsymbol{S}'/\nu^3$.

4.1 Transformation to locally-flat co-moving frame

The angle χ in the expression (53), θ in the response tensor, and similar quantities need to either be evaluated in the locally-flat reference frame, where fluid is at rest, or properly calculated in GR. We choose the first path as a transparent one with the following recipe. First, one traces the null geodesic from the observer's plane to the BH horizon or the sphere far from the BH and finds the vectors k^α and a^α (see eqs.(56,58)). At each point on the ray one knows the vectors k^α, a^α, fluid four-velocity u^α, and the four-vector of magnetic field B_0^α defined in McKinney & Gammie (2004) in lab frame. The next step is to transform all vectors to the co-moving frame. Let us construct an orthonormal basis in Kerr metric in lab frame

$$\begin{gathered} e^\alpha_{(t)} = (u^t, u^r, u^\theta, u^\phi), \\ e^\alpha_{(r)} \propto (u^t u_r, -(u^t u_t + u^\phi u_\phi), 0, u^\phi u_r), \\ e^\alpha_{(\theta)} \propto (u^t u_\theta, u^r u_\theta, u^\theta u_\theta + 1, u^\phi u_\theta), \\ e^\alpha_{(\phi)} \propto (-u_\phi/u_t, 0, 0, 1), \end{gathered} \quad (63)$$

where lower-index velocity is $u_\alpha = g_{\alpha\beta}u^\beta$ and $g_{\alpha\beta}$ is the lower index Kerr metric

$$g_{\alpha\beta} = \begin{pmatrix} -1+\frac{2r}{\rho} & 0 & 0 & -\frac{2ar\sin^2\theta_a}{\rho} \\ 0 & \rho/\Delta & 0 & 0 \\ 0 & 0 & \rho & 0 \\ -\frac{2ar\sin^2\theta_a}{\rho} & 0 & 0 & \frac{\Sigma\sin^2\theta_a}{\rho} \end{pmatrix} \quad (64)$$

in (t, r, θ_a, ϕ) spherical polar coordinates with polar angle θ_a, radius r, spin a, $\rho = r^2 + a^2\cos^2\theta_a$, $\Delta = r^2 - 2r + a^2$, $\Sigma = (r^2+a^2)^2 - a^2\Delta\sin^2\theta_a$. Then make a transformation to

$$\begin{aligned} \hat{e}^\alpha_{(t)} &= (1,0,0,0), \\ \hat{e}^\alpha_{(r)} &= (0,1,0,0), \\ \hat{e}^\alpha_{(\theta)} &= (0,0,1,0), \\ \hat{e}^\alpha_{(\phi)} &= (0,0,0,1) \end{aligned} \quad (65)$$

via

$$S_{(t,r,\theta,\phi)\beta} = (-e^\alpha_{(t)}, e^\alpha_{(r)}, e^\alpha_{(\theta)}, e^\alpha_{(\phi)})g_{\alpha\beta}. \quad (66)$$

The transformation of a four-vector A^β to the co-moving frame is then

$$\hat{A}_{(t,r,\theta,\phi)} = S_{(t,r,\theta,\phi)\beta}A^\beta. \quad (67)$$

The metric in the new frame

$$S_{(i)\alpha}g^{\alpha\beta}(S_{(k)\beta})^T = \eta_{ik} \quad (68)$$

coincides with Minkowski metric $\eta_{ik} = \mathrm{diag}(-1,1,1,1)$. The velocity four-vector u^β transforms to $\hat{u}_{(i)} = (1,0,0,0)^T$. Thus, the basis change (67) with matrix (66) and vectors (63) constitutes the transformation to the locally-flat co-moving reference frame. This procedure is the alternative of the numerical Gramm-Schmidt orthonormalization applied in Moscibrodzka et al. (2009). Note, that despite the vectors (63) do not explicitly depend on the metric elements, the expressions rely on the properties of Kerr metric and are not valid for general $g^{\alpha\beta}$.

Upon transforming u^α, k^α, a^α, B_0^α to the co-moving frame we easily find the wave frequency $\nu = -\hat{k}_{(0)}$, then $\hat{\boldsymbol{k}} = \hat{k}_{(1,2,3)}$. The perpendicular vector $\hat{\boldsymbol{a}}$ needs to be offset by $\hat{\boldsymbol{k}}$ as

$$\hat{\boldsymbol{a}} = \hat{a}_{(1,2,3)} - \hat{\boldsymbol{k}}\frac{\hat{a}_{(0)}}{\hat{k}_{(0)}} \quad (69)$$

and then normalized to construct a spatial unit vector. The offset is due to the enforcement of Lorenz gauge (12). It conveniently makes $\boldsymbol{a}\cdot\boldsymbol{k} = \hat{\boldsymbol{a}}\cdot\hat{\boldsymbol{k}} = 0$. The vector $\boldsymbol{b}$ is found by a simple vector product

$$\hat{\boldsymbol{b}} = \hat{\boldsymbol{a}} \times \hat{\boldsymbol{k}} \quad (70)$$

and then normalized. The spatial part ($\hat{\boldsymbol{e}}_{(r)}$, $\hat{\boldsymbol{e}}_{(\theta)}$, $\hat{\boldsymbol{e}}_{(\phi)}$) of basis (65) relates to basis ($\boldsymbol{e}^1$, $\boldsymbol{e}^2$, $\boldsymbol{e}^3$) via the orthonormal transformation preserving angles. The magnetic field B_0^α gets transformed to a three-vector $\hat{\boldsymbol{B}}_0$ and all the angles are found in correspondence to Fig. 1 with the help of equations (52,53) applied to hatted vectors. For example, $\cos\theta = (\hat{\boldsymbol{k}}\cdot\hat{\boldsymbol{B}}_0)/(\hat{k}\hat{B}_0)$. Then the whole matrix $\hat{\mathbf{K}}$ is found.

5 APPLICATION TO COMPACT OBJECTS

The described GR polarized radiative transfer finds its application in accretion onto low luminosity active galactic nuclei (LLAGNs), in particular Sgr A*. The application of GR is necessary to infer the BH spin, which provides important information on the past evolution of the BH and the host galaxy itself. For example, the accretion efficiency in the AGN phase depends strongly on the value of BH spin (Shapiro 2005). The value of spin and spin orientation constraints the accretion and merger history (Rees & Volonteri 2007).

The detailed application to Sgr A* will be reported elsewhere (Shcherbakov & Penna (2010), in prep.). Here we describe only the effects, which help to produce the observed cyclo-synchrotron spectra, linear (LP) and circular (CP) polarization fractions, and the electric vector position angle (EVPA) as functions of frequency. The effects are plenty, what proves it hard to disentangle and provide simple explanations of observations. It is in general challenging to achieve the realistic level of details in collisionless plasma modelling.

First, the radiation from LLAGNs appears to be variable in time. The simultaneous short observations can provide only the single snapshot of a system, not necessarily representative of a long term behavior. Thus, it is necessary to obtain the statistically significant sample of variability of both observed and simulated spectra to reliably estimate the average or typical flow parameters and BH spin. As recent research suggests (Dodds-Eden et al. 2010), the modelling of a single flare can successfully be done even without invoking GR.

As in the case of Sgr A*, the cyclo-synchrotron specific flux F_ν vs ν can have a peak. The peak frequency ν^* and flux F_ν^* do not necessarily correspond to the thermal cut-off of emission. Even a small percentage of the non-thermal electrons can radiate significantly more than the bulk of thermal electrons. For the efficient particle acceleration most of emission may come from the energetic electrons with cooling time $t_{\rm cool}$ about the time of inflow $t_{\rm in}$ from several BH gravitational radii $r_{\rm g} = 2GM/c^2$. The gravitational redshift and Doppler shift due to relativistic motion can strongly modify the peak ν^* and F_ν^*.

The LP fraction can provide constraints on flow density near the emitting region owing to beam depolarization effect. The LP fraction is the highest at high frequencies, where only a small region of the flow shines and beam depolarization is weak. As all regions of the flow radiate at lower frequencies, differential Faraday rotation and emission EVPA vary, the resultant LP fraction is subject to cancelations and quickly ceases with ν. However, cancelations at high ν may readily happen between two regions with similar fluxes and perpendicular EVPAs, those regions would have perpendicular magnetic fields.

The same change of EVPA with frequency can mimic the Faraday rotation. The finite rotation measure (RM)

$$RM = \frac{EVPA_1 - EVPA_2}{\lambda_1^2 - \lambda_2^2} \quad (71)$$

does not necessarily happen due to Faraday rotation $\sim \int n\boldsymbol{B}\cdot\boldsymbol{dl}$. Here $\lambda = c/\nu$ is the wavelength. In fact, the meaningful application of formula (71) is limited to a toy case of cold plasma far from the emitting region with the homogeneous magnetic field. In reality, besides the change of emission EVPA with ν, the Faraday rotation coefficient $\rho_V(\nu)$ is a function of frequency (Shcherbakov 2008). The differential rotation measure

$$dRM = dEVPA/d(\lambda^2) \quad (72)$$

is the measured quantity (Marrone et al. 2007). It should be used in constraining the models. Also, significant Faraday rotation can happen in the emitting region, what introduces the effect of differential optical depth. Thus, one can only fit the observed EVPA(ν) and use it along with other observables to constrain the system free parameters. As $\rho_V(\nu)$ is a steeply declining function of temperature θ_e (Shcherbakov 2008), the relativistic charges contribute little to this quantity.

Substantial levels of circular polarization were recently found in Sgr A* (Munoz et al. (2010), in prep.). There are several effects producing finite CP. First recognized was the emissivity ε_V in V mode. According to Melrose (1971) it only is a factor of γ weaker than the total emissivity ε_I. It produces the largest V along the magnetic field. The

Faraday conversion, transformation between the linear polarization and the circular, operates perpendicular to the magnetic field. The Faraday conversion coefficient ρ_Q has a peculiar dependence on temperature of thermal plasma or particles' γ-factor (Shcherbakov 2008): $\rho_Q = 0$ for cold plasma, ρ_Q is exponentially inhibited for very hot plasma and reaches the maximum for transrelativistic plasma with $\theta_e \sim \gamma \sim$ several $\cdot\, mc^2/k_B$. The exponential inhibition is an effect of finite ratio ν/ν_B with peak ρ_Q only around $\theta_e \sim 10$ for $\nu/\nu_B \sim 10^3$. Thus, for hot bulk part of particle distribution with $\gamma \sim$ several $\cdot\, mc^2/k_B$ the non-thermal electrons do not contribute significantly to Faraday conversion. Note that this result supersedes Ballantyne, Ozel & Psaltis (2007), who following Melrose (1997) neglected the importance of finite ratio ν/ν_B. Similarly to linear polarization, the beam depolarization can lower the net value of circular polarization at low frequencies due to differential Faraday conversion.

In sum, there are often several explanations for the same observable quantity. One should not settle for a simplified model trying to reproduce the observations. Instead, the rigorous ray tracing and aposteriori explanations of a fit to the observables would be the preferred reliable way.

6 DISCUSSION & CONCLUSIONS

In our endeavor to provide the complete and self-consistent description of GR polarized radiative transfer we conduct the full derivation starting from definitions and basic equations. The goal is to make the easy, transparent, and error-free derivations, thus Mathematica 7 was used underway, the expressions were cross-checked. The absorptivities for thermal plasma were checked numerically against known synchrotron emissivities and cyclo-synchrotron approximations in Sazonov (1969); Leung, Gammie & Noble (2009). We stepped away from the standard textbooks and assumed "the opposite" observers' definition of circular polarization V, carrying the definition through all other calculations. We chose the coordinate system with coplanar $\boldsymbol{k}$, $\tilde{\boldsymbol{e}}^2$, $\boldsymbol{B}_0$ and derived the plasma response tensor $\tilde{\alpha}_{ik}$ in $(\tilde{\boldsymbol{e}}^1, \tilde{\boldsymbol{e}}^2, \tilde{\boldsymbol{e}}^3)$ basis, also projecting it onto the transverse coordinates $\boldsymbol{e}^1$, $\boldsymbol{e}^2$. Repeating for completeness Huang et al. (2009), we tie the polarized radiative transfer equation in the latter coordinates (17) with the transfer in $\boldsymbol{a}$, $\boldsymbol{b}$ coordinates with the help of matrix (50). The generalization of radiative transfer to GR is performed in the easiest way owing to the invariance of occupation numbers in different photon states and the invariance of the transformation between the states. Lorenz gauge (12) helps to establish the correspondence between 4×4 and spatial 3×3 quantities and to correctly find the transverse vectors $\boldsymbol{a}$, $\boldsymbol{b}$ in the co-moving locally-flat reference frame. The transformation from the lab frame with Kerr metric to that frame is explicitly given. The intricacies of application of GR polarized radiative transfer to LLAGNs are discussed. As the transfer incorporates many physical effects, a priori guessing of the most important effects is discouraged in favor of full calculation. The provided interface of dynamical models and observations is waiting for its applications.

The treatment of particles distributions is still limited. In the current state the calculations are optimized for isotropic in pitch-angle distributions and become especially simple for thermal particle distribution. The integration over the pitch-angle in formula (35) is in general impossible to perform for non-isotropic distributions. In this case, the integral over ξ should be done first analytically. This calculation is left for future work.

ACKNOWLEDGMENTS

The authors are grateful to Charles Gammie, James Moran, Diego Munoz, and Ramesh Narayan for fruitful discussions, Akshay Kulkarni and Robert Penna for help with the transformation to the locally-flat co-moving frame. Charles Gammie kindly provided us a draft of their paper (Gammie et al. (2010), in prep.) on covariant formalism of polarized ray tracing.

The work is partially supported by NASA grant NNX08AX04H to RVS and China Postdoctoral Science Foundation grant 20090450822 to LH.

REFERENCES

Anile A. M., Breuer R. A., 1974, ApJ, 189, 39
Ballantyne D. R., Ozel F., Psaltis D., 2007, ApJ, 663, L17
Broderick A., 2004, Ph.D. thesis, California Institute of Technology
Chan C.-K., Liu S., Fryer C. L., Psaltis D., O"zel F., Rockefeller G., Melia F., 2009, ApJ, 701, 521
Dodds-Eden K., Sharma P., Quataert E., Genzel R., Gillessen S., Eisenhauer F., Porquet D., 2010, ApJ, submitted
Ellis G. F. R., 2009, Rel. Cosmology, 41, 581
Gammie C. F. et al., 2010, in preparation
Hamaker J. P., Bregman J. D., 1996, A & AS, 117, 161
Hawley J. F., Balbus, S. A., 2002, ApJ, 573, 738
Huang L., Shcherbakov R., 2010, in preparation
Huang L., Liu S., Shen Z.-Q., Yuan Y.-F., Cai M. J., Li H., Fryer C. L., 2009, ApJ, 703, 557
Igumenshchev I. V., Narayan R., 2002, ApJ, 566, 137
Landau L. D., Lifshitz E. M., 1975, "Classical theory of fields", (Oxford: Pergamon Press)
Landau L. D., Lifshits E. M., 1980, "Physical Kinetics" (Oxford: Pergamon Press)
Legg M. P. C., Westfold K. C., 1968, ApJ, 154, 499
Leung P. K., Gammie C. F., Noble S. C., 2009, ApJ, submitted
McKinney, J. C., Gammie, C. F. 2004, ApJ, 611, 977
Marrone D. P., Moran J. M., Zhao J., Rao R., 2007, ApJ, 654, L57
Melrose D. B., 1971, Ap&SS, 12, 172
Melrose D. B., 1997, J. Plasma Physics, 58, 735
Melrose D. B., McPhedran R. C., 1991, "Electromagnetic Processes in Dispersive Media", (Cambridge University Press: Cambridge)
Mihalas D., Mihalas B. W., 1984, "Foundations of radiation hydrodynamics", (New York: Oxford University Press)
Misner C. W., Thorne K. S., Wheeler J. A., 1973, "Gravitation", (San-Francisco: Freeman and Company)
Moscibrodzka M., Gammie C. F., Dolence J. C., Shiokawa H., Leung P. K., 2009, ApJ, 706, 497
Munoz D. et al., 2010, in preparation

Pacholczyk A. G., 1970, "Radio astrophysics. Nonthermal processes in galactic and extragalactic sources", (Freeman: San Francisco)

Rees M. J., Volonteri M., 2007, proceedings to "Black Holes from Stars to Galaxies" (editor: V. Karas), p. 51

Rochford K., 2001, book chapter in "Encyclopedia of Physical Science and Technology", (Academic press)

Ruffert M., 1994, ApJ, 427, 342

Rybicki G. B., Lightman A. P., 1979, "Radiative processes in astrophysics", (Wiley-Interscience: New York)

Sazonov V. N., 1969, Soviet Astronomy, 13, 396

Sazonov V. N., Tsytovich V. N., 1968, Radioph. and Quant. Electr., 11, 731

Shafee R., McKinney J. C., Narayan R., Tchekhovskoy A., Gammie C. F., McClintock J. E., 2008, ApJ, 687, L25

Shapiro S. L., 2005, ApJ, 620, 59

Shcherbakov R. V., 2008, ApJ, 688, 695

Shcherbakov R. V., Penna R. F., 2010, in preparation

Sironi L., Spitkovsky A., 2009, ApJ, 707, L92

Swanson D. G., 2003, "Plasma waves" (Bristol: Institute of Physics Pub.)

Trubnikov B. A., 1958, "Magnetic emission of high temperature plasma". Thesis, Moscow Institute of Engineering and Physics [English translation in AEC-tr-4073, US Atomic Energy Commission, Oak Ridge, Tennessee, 1960]. B.A. Trubnikov.

Wilson T. L., Rohlfs K., Huttemeister S., 2009, "Tools of Radio Astronomy", (Springer: Berlin)